

Reconsidering the Performance of GAE in Link Prediction

Weishuo Ma

School of Electronics Engineering and Compute Science,
Peking University
Haidian Qu, Beijing Shi, China
2200013081@stu.pku.edu.cn

Xiyuan Wang

Institute for Artificial Intelligence, Peking University
Haidian Qu, Beijing Shi, China
wangxiyuan@pku.edu.cn

Yanbo Wang

Institute for Artificial Intelligence, Peking University
Haidian Qu, Beijing Shi, China
wangyanbo@stu.pku.edu.cn

Muhan Zhang*

Institute for Artificial Intelligence, Peking University
Haidian Qu, Beijing Shi, China
muhan@pku.edu.cn

ABSTRACT

Recent advancements in graph neural networks (GNNs) for link prediction have introduced sophisticated training techniques and model architectures. However, reliance on outdated baselines may exaggerate the benefits of these new approaches. To tackle this issue, we systematically explore Graph Autoencoders (GAEs) by applying model-agnostic tricks in recent methods and tuning hyperparameters. We find that a well-tuned GAE can match the performance of recent sophisticated models while offering superior computational efficiency on widely-used link prediction benchmarks. Our approach delivers substantial performance gains on datasets where structural information dominates and feature data is limited. Specifically, our GAE achieves a state-of-the-art Hits@100 score of 78.41% on the ogbl-ppa dataset. Furthermore, we examine the impact of various tricks to uncover the reasons behind our success and to guide the design of future methods. Our study emphasizes the critical need to update baselines for a more accurate assessment of progress in GNNs for link prediction. Our code is available at <https://github.com/GraphPKU/Refined-GAE>.¹

CCS CONCEPTS

• Computing methodologies → Neural networks; • Mathematics of computing → Graph algorithms.

KEYWORDS

Graph Neural Networks, Link Prediction, Graph Autoencoders

ACM Reference Format:

Weishuo Ma, Yanbo Wang, Xiyuan Wang, and Muhan Zhang. 2018. Reconsidering the Performance of GAE in Link Prediction. In *Proceedings*

*Correspondence is to Muhan Zhang

¹This paper has been accepted for presentation at the 34th ACM International Conference on Information and Knowledge Management (CIKM 2025).

Permission to make digital or hard copies of all or part of this work for personal or classroom use is granted without fee provided that copies are not made or distributed for profit or commercial advantage and that copies bear this notice and the full citation on the first page. Copyrights for components of this work owned by others than the author(s) must be honored. Abstracting with credit is permitted. To copy otherwise, or republish, to post on servers or to redistribute to lists, requires prior specific permission and/or a fee. Request permissions from permissions@acm.org.

Conference acronym 'XX, June 03–05, 2018, Woodstock, NY

© 2018 Copyright held by the owner/author(s). Publication rights licensed to ACM.

ACM ISBN 978-1-4503-XXXX-X/2018/06...\$15.00

<https://doi.org/XXXXXXX.XXXXXXX>

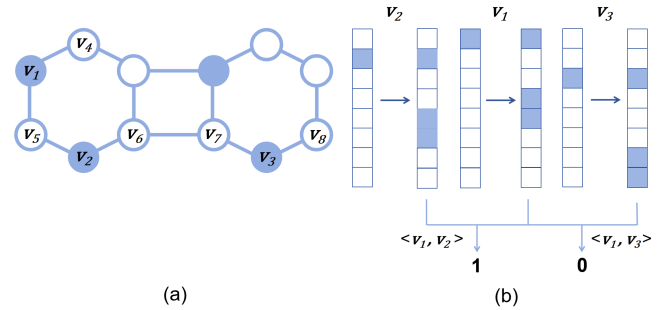


Figure 1: (a) illustrates An example of the limitations of GAE. Although v_2 and v_3 share the same representation due to symmetry, the pair (v_1, v_2) should be represented differently from (v_1, v_3) . (b) demonstrates how GAE counts common neighbors by performing inner products on the linear combinations of neighboring one-hot embeddings.

of Make sure to enter the correct conference title from your rights confirmation email (Conference acronym 'XX). ACM, New York, NY, USA, 12 pages. <https://doi.org/XXXXXXX.XXXXXXX>

1 INTRODUCTION

Link prediction is a fundamental problem in graph learning with applications in recommendation systems [35], drug discovery [23], and knowledge graphs [38]. GNNs have achieved strong performance in these domains and are widely adopted for link prediction tasks. Among GNNs, GAE [10] is a well-known model that predicts link probabilities by computing inner products of node representations learned through a Message Passing Neural Network (MPNN).

However, Zhang and Chen [34] found that GAE's expressiveness is limited. For example, as illustrated in Figure 1a, GAE produces identical predictions for links (v_1, v_2) and (v_1, v_3) , despite their differing structural contexts. This limitation arises because GAE computes node representations independently, disregarding the structural relationships between nodes. To address this challenge, various methods have been proposed to enhance expressiveness and better capture graph structure, such as labeling tricks [34], paths between nodes [38], and neighborhood overlaps [3, 14, 26, 32]. These approaches often introduce complex designs with increased time and space complexity, claiming superior performance. Although expressiveness improvement caused by architecture changes is important, **we observe that holistic optimization of existing**

GAE components and meticulous hyperparameter tuning also contribute significantly to these models' success.

This observation motivates a fair re-evaluation: baseline GAEs must also be applied with such optimization to be compared with extensively tuned models. We therefore reimplemented GAE, systematically applying principled, relatively simple enhancements and meticulous hyperparameter tuning, practices common in modern GNN development. Our approach also introduces a flexible input strategy and key architectural optimizations. These empirical efforts are supported by theoretical analysis; this analysis of GAE with linear propagation and unique inputs reveals an inherent capacity for processing pairwise neighborhood information, akin to capturing generalized common neighbor information. The theoretical grounding, further reinforced by empirical findings such as trained learnable embeddings tending to remain near-orthogonal, validates the effectiveness achieved through optimized GAE.

Through extensive experiments on Planetoid [21] and Open Graph Benchmark [9] datasets, we demonstrate that **properly Optimized GAE, with its core simplicity largely intact, can match or surpass SOTA models.** As detailed in Table 2, our Optimized GAE achieves **top-two** performance on all listed datasets and attains the leading average rank compared against all baselines, notably yielding an average improvement of **6.4%** over the strongest NCN baseline [26]. **Notably, it establishes a new SOTA Hits@100 score of 78.41% on the large-scale ogbl-ppa dataset.** These results demonstrate that an optimized GAE model can serve as a powerful and more efficient alternative, comparable to complex GNN architectures that explicitly inject pairwise information. The general applicability of these optimization principles is confirmed by similar performance improvements when applied to NCN [26]. This highlights the benefits of a carefully refined base model. Finally, comprehensive ablation studies validate the contribution of each design choice of GAE, providing valuable observations to guide the future development of link prediction models.

In conclusion, we re-evaluate GAE in this study, delivering a stronger baseline for future endeavors. Our main contributions are:

- We demonstrate that a GAE model with systematic optimization can achieve link prediction performance competitive with, or even better than, SOTA models. This finding shows that systematic optimization of simpler architectures can yield strong results, supporting the critical re-evaluation of basic models to establish more effective and efficient baselines in the field.
- We provide a comprehensive analysis of the crucial design choices and optimization strategies spanning input representation, architectural configurations, and hyperparameter tuning. We detail their effects to offer actionable guidelines for the development of efficient and powerful link prediction models.

2 RELATED WORKS

GNNs for Link Prediction. Traditional link prediction methods such as Common Neighbors (CN) [2], Adamic-Adar (AA) [1], and Resource Allocation (RA) [36] use fixed heuristics based on shared neighbors. These methods are efficient for capturing local graph

structures but are less effective when dealing with complex relationships on diverse datasets. GNNs overcome these issues by learning node representations directly from data.

The GAE [10], an early GNN-based method, uses an MPNN to generate node embeddings and predicts links using inner product similarity. However, its expressiveness is limited because it does not explicitly model pairwise relationships. To address this, SEAL [34] improves expressiveness by extracting and processing local sub-graphs around target links with a GNN. Neo-GNN [32] and BUDDY [3] process the entire graph, using higher-order common neighbor information for improved global modeling. NCN [26] further develops pairwise modeling by learning embeddings for common neighbors instead of using manually defined features. Other research has focused on generalizing heuristic methods. NBFNet [38] unifies path-based heuristics using the Bellman-Ford algorithm, while Mao et al. [18] categorizes heuristics into local and global ranges for broader structural modeling. LPFormer [22] uses an adaptive transformer to dynamically select relevant heuristics for each dataset. Similarly, Link-MOE [17] uses an ensemble of link predictors to flexibly combine multiple heuristics.

Research has also addressed data-related challenges affecting link prediction. For example, LTLP [28] reduces bias from long-tailed distributions to improve performance on imbalanced datasets. Zhu et al. [37] studied the impact of homophily and heterophily.

Baseline Evaluation and Optimization in GNNs. As new GNN models are introduced, recent studies suggest caution with evaluation practices that might exaggerate the benefits of complex models. For link prediction, Li et al. [12] identified key problems such as poorly tuned baselines and unrealistic negative sampling in evaluations, which can hide the true performance differences between models. Similar concerns exist in other graph tasks. Luo et al. [15] showed that classic GNNs with carefully tuned under standard methods can perform even better than complex Graph Transformers. This applies to node-level [15] and graph-level tasks [16]. These findings question the assumption of the necessity of complex architectures.

3 PRELIMINARIES

Notation. We consider an undirected graph $G = (V, E, X)$, where V is a set of n nodes, E is the set of edges, and $X \in \mathbb{R}^{n \times d}$ is the d -dimensional node feature matrix. Let A be the adjacency matrix. The set of neighbors for node i is $\mathcal{N}(i) = \{j \in V \mid A_{ij} > 0\}$. The shortest path distance between i and j is $\text{dist}(i, j)$. The k -hop neighborhood of node i , $\mathcal{N}_k(i)$, includes all nodes j such that $\text{dist}(i, j) \leq k$.

GAE. GAEs [10] are a type of model used for link prediction. GAEs learn low-dimensional node embeddings that preserve graph structure and node attributes. These embeddings are then used to predict link likelihoods. A GAE has two main components:

Encoder: The encoder uses a MPNN to map node features and graph topology to latent embeddings, which can be formulated as:

$$Z = \text{Encoder}(A, X). \quad (1)$$

A common encoder is the Graph Convolutional Network (GCN) [11]. Its layer-wise propagation rule is:

$$Z^{(l+1)} = \sigma \left(\tilde{D}^{-1/2} \tilde{A} \tilde{D}^{-1/2} Z^{(l)} W^{(l)} \right), \quad (2)$$

where $Z^{(l)}$ is the matrix of node embeddings at layer l , $\tilde{A} = A + I_n$ is the adjacency matrix with self-loops, \tilde{D} is the degree matrix of \tilde{A} , $W^{(l)}$ is a trainable weight matrix, and σ is an activation function.

Decoder: The decoder uses the latent embeddings Z to reconstruct the adjacency matrix A or predict edge likelihoods. For link prediction, a common approach is to compute the probability of an edge (i, j) using the dot product of their embeddings:

$$\hat{A}_{ij} = \sigma_{\text{sig}}(Z_i^T Z_j), \quad (3)$$

where \hat{A}_{ij} is the predicted probability of an edge, Z_i and Z_j are the latent embeddings of nodes i and j , and σ_{sig} is the sigmoid function.

The GAE is trained by minimizing an objective function, commonly the binary cross-entropy (BCE) loss. This loss is calculated over a set of positive edges E_{pos} (from E) and a set of sampled negative edges E_{neg} (node pairs not in E). Let $N_{\text{total}} = |E_{\text{pos}}| + |E_{\text{neg}}|$, and the BCE loss \mathcal{L} is then:

$$\mathcal{L} = -\frac{1}{N_{\text{total}}} \left(\sum_{(i,j) \in E_{\text{pos}}} \log \hat{A}_{ij} + \sum_{(i,k) \in E_{\text{neg}}} \log(1 - \hat{A}_{ik}) \right). \quad (4)$$

4 OPTIMIZING GAES FOR LINK PREDICTION

The GAE architecture, while a common starting point for link prediction, has well-known limitations in its expressiveness. This section addresses these known constraints by carefully re-evaluating GAE's inherent abilities and showing systematic ways to improve its empirical performance. We begin by theoretically re-examining GAE's core architecture, which reveals an often overlooked ability to process pairwise neighborhood information. Subsequently, using these insights and applying principles of holistic optimization, we introduce the Optimized GAE framework. We detail the systematic design choices and tuning strategies that significantly improve link prediction performance. The specific impact of these design choices is validated in our ablation studies (Section 5.3).

4.1 GAE's Inherent Pairwise Structure Modeling

To re-examine the GAE architecture for link prediction, it is important to first consider how its expressiveness is typically assessed. Standard analyses often evaluate GNNs, including GAE, by assuming permutation-invariant initial node labels. Under such conditions, these analyses show that GAE's ability to distinguish graphs is similar to the 1-WL test. This highlights a basic limitation in its ability to process purely structural information [19, 34].

However, GAE applications for link prediction typically use non-permutation-invariant inputs, departing from the assumption of uniform initial labeling. This key difference arises in two main ways: nodes may have unique features, or unique initial embeddings (learnable or distinctly initialized) are used. Either approach gives each node a unique starting signature. This fundamentally changes the GAE's operating conditions compared to those assumed in analyses that rely on initial permutation invariance. Our theoretical exploration of GAE's pairwise processing ability starts from this practical consideration.

For analytical clarity, we consider a simple GAE variant. Its encoder has k linear GNN layers that operate on input node features $\mathbf{X} \in \mathbb{R}^{n \times d}$. The resulting node embeddings $\mathbf{Z} \in \mathbb{R}^{n \times d}$ are:

$$\mathbf{Z} = f_{\text{enc}}(\mathbf{A}, \mathbf{X}) = \tilde{\mathbf{A}}^k \mathbf{X}, \quad (5)$$

with $\tilde{\mathbf{A}}$ being the normalized adjacency matrix. Using a dot product decoder, the logit for a link (i, j) is $\mathbf{z}_i^T \mathbf{z}_j$. Node i 's embedding \mathbf{z}_i is a weighted sum of features from its k -hop neighborhood $N_k(i)$:

$$\mathbf{z}_i = \sum_{p \in N_k(i)} \alpha_{ip} \mathbf{x}_p, \quad (6)$$

where $\alpha_{ip} = (\tilde{\mathbf{A}}^k)_{ip}$ is the weight and $\mathbf{x}_p \in \mathbb{R}^d$ is the initial feature vector of node p . Similarly, node j 's embedding is $\mathbf{z}_j = \sum_{q \in N_k(j)} \beta_{jq} \mathbf{x}_q$, with $\beta_{jq} = (\tilde{\mathbf{A}}^k)_{jq}$. The dot product is:

$$\begin{aligned} \text{logit}(i, j) &= \left(\sum_{p \in N_k(i)} \alpha_{ip} \mathbf{x}_p \right)^T \left(\sum_{q \in N_k(j)} \beta_{jq} \mathbf{x}_q \right) \\ &= \sum_{p \in N_k(i)} \sum_{q \in N_k(j)} \alpha_{ip} \beta_{jq} (\mathbf{x}_p^T \mathbf{x}_q). \end{aligned} \quad (7)$$

This expansion shows how the GAE score for a potential link (i, j) is formed. The terms in Equation 7 where $p = q$ (representing a shared node, which we denote by r) sum to $\sum_{r \in N_k(i) \cap N_k(j)} \alpha_{ir} \beta_{jr} \|\mathbf{x}_r\|_2^2$. This reflects the influence of these shared nodes r , weighted by their initial feature norms. This becomes particularly clear if the initial node embeddings \mathbf{x}_r are orthogonal (e.g., $\mathbf{x}_p^T \mathbf{x}_q \approx 0$ for $p \neq q$) and have approximately unit norm ($\|\mathbf{x}_r\|_2^2 \approx 1$). In such cases, the logit approximately simplifies to $\text{logit}(i, j) \approx \sum_{r \in N_k(i) \cap N_k(j)} \alpha_{ir} \beta_{jr}$. For $k = 1$, this sum is $(\tilde{\mathbf{A}}^2)_{ij}$, which is a weighted **common neighbor count** between nodes i and j (since $\alpha_{ir} = (\tilde{\mathbf{A}})_{ir}$ and $\beta_{jr} = (\tilde{\mathbf{A}})_{jr}$). This way of obtaining common neighbor information from propagated orthogonal inputs is also discussed by Dong et al. [5] (illustrated in Figure 1b). More generally, for propagation depth k , the sum $\sum_r (\tilde{\mathbf{A}}^k)_{ir} (\tilde{\mathbf{A}}^k)_{jr} = (\tilde{\mathbf{A}}^{2k})_{ij}$ captures higher-order path overlaps. **Thus, GAES, especially with unique orthogonal inputs, inherently capture signals similar to generalized common neighbor information, a key factor for link prediction.**

Furthermore, the terms in Equation 7 where $p \neq q$ involve dot products $(\mathbf{x}_p^T \mathbf{x}_q)$ between initial features of different nodes p (in $N_k(i)$) and q (in $N_k(j)$). If these initial features \mathbf{x}_p are general (or are learnable embeddings that develop non-zero dot products for $p \neq q$), these terms measure feature similarity between different nodes. For example, strong positive feature correlations between nodes near i and nodes near j might suggest shared community traits. In contrast, feature dissimilarities could indicate contexts less favorable for a link. This ability to assess interactions between different nodes in their neighborhoods allows the model to consider more than just shared nodes, but local environments comprehensively. **Considering these cross-neighborhood feature similarities is thus crucial, as it allows the model to assess the overall compatibility between the environments of nodes i and j .**

In conclusion, using unique initial node features or embeddings allows GAES to inherently perform complex pairwise information processing. They can therefore effectively capture common neighbor signals and assess node environment compatibility, offering more detailed insights for link prediction. This perspective complements traditional analyses of expressiveness that focus on purely structural information.

4.2 Design Choices for Enhanced GAE

This section details key architectural design choices for GAEs. The design principles are based on theoretical insights, and their effectiveness is empirically validated in Section 5.3.

4.2.1 Input Nodes Representations. The insights from Section 4.1 guide our approach to designing input node representations. The main decision for initial node representations is whether to use raw node features alone, or to combine them with learned node embeddings. This choice primarily depends on two key factors: first, **the relative predictive power of inherent node features versus the graph's structure**, and second, **the overall size and density of the graph**. Carefully evaluating these factors is important for choosing an input strategy that maximizes GAE performance.

To formally measure the relative influence of structure versus features for a dataset D and a link prediction evaluation metric M , we consider the performance of simple, deterministic link heuristics. Let $P_S(D, M)$ be the performance of a heuristic that relies *exclusively* on graph structure (e.g., Common Neighbors [2]). Similarly, let $P_F(D, M)$ be the performance of a heuristic using *only* node features (e.g., the cosine similarity of features). A **Structure-to-Feature Dominance Index** ($I_{S/F}$) can then be defined as:

$$I_{S/F}(D, M) = \frac{P_S(D, M)}{P_S(D, M) + P_F(D, M) + \epsilon} \quad (8)$$

where ϵ is a small constant to ensure numerical stability if both P_S and P_F are zero. This index, ranging from approximately 0 to 1, offers a principled way to measure the reliance on structure or feature: an $I_{S/F}$ value close to 1 signifies **structural reliance**, suggesting that topology is the main factor for link formation. Conversely, an $I_{S/F}$ approaching 0 indicates **feature reliance**. An index around 0.5 suggests a balance, or that neither structure nor features alone are sufficient. **This $I_{S/F}$ index provides a quantitative basis for tailoring the GAE's input strategy.**

The $I_{S/F}$ index, along with graph size and density, guides the choice of input representation. A low $I_{S/F}$ favors using raw features if available, while a high $I_{S/F}$ suggests learnable embeddings are needed. The suitability of learnable embeddings then depends on the **number of nodes** (n) and the **average degree**. A higher average degree translates to more per-node connections, enriching the relational data available for training each node's d -dimensional embedding. For large graphs, fixed-capacity encoders and decoders may struggle to adequately represent the vast number of individual nodes, where learnable embeddings become crucial for boosting model capacity. When a graph is both large and dense, the extensive parameters of learnable embeddings are better supported, which helps mitigate the risk of overfitting that can be more pronounced in sparser or smaller graphs. **Therefore, the optimal input strategy involves a careful synthesis of the $I_{S/F}$ index, the number of nodes, and the average degree.**

When using learnable embeddings, their initialization is an important next step. Orthogonal initialization stands out as a reliable and theoretically sound starting point. As demonstrated in Section 4.1, such initialization allows the GAE's predictive score to directly reflect measures similar to **weighted common neighbor counts**. By setting the initial dot product between distinct node pairs to zero, this approach creates an unbiased starting point, assuming

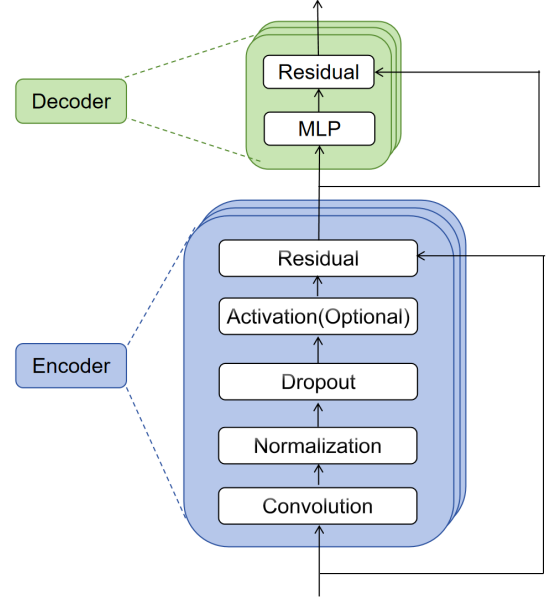


Figure 2: A visual overview of a typical GAE architecture, highlighting the encoder and decoder modules.

no arbitrary initial correlations. Later, the model can learn meaningful node embeddings whose pairwise dot products can capture important correlations. **Therefore, orthogonal initialization for learnable embeddings is very helpful for link prediction.**

4.2.2 Key Architectural Modules of Graph Autoencoders. Following the principled approach for selecting input representations from Section 4.2.1, we now focus on the GAE's internal architecture. Figure 2 provides a visual overview of this typical architecture. We will now examine the specific components: how the encoder refines embeddings and how the decoder uses them to predict link scores.

The **encoder's** role is to transform the input graph structure and the chosen initial node embeddings into lower-dimensional latent embeddings. This is typically achieved using a stack of MPNN layers. Key operations and components in these MPNN layers include:

Convolutional Layer. Convolutional layers are important for determining how node information is aggregated, and their design can significantly affect the model's sensitivity to graph structures. Here, we focus on several commonly used architectures—GCN [11], GraphSAGE [6], GAT [24], and GIN [31]—that each use unique methods for feature aggregation. Table 1 summarizes their different strengths and weaknesses. Among them, GCN is notable for its balanced approach to handling varying node degrees, which makes it both robust and efficient across datasets. **We use GCN as the primary architecture in our main experiments.**

Residual Connections. Residual connections [7] are important in deep learning for addressing vanishing gradients and improving training stability. While MPNNs often include self-loops, which offer an implicit way to keep original information, we find it is still helpful to use an **initial residual**. This design explicitly sums the *original* node features ($Z^{(0)}$) with the output of *each* MPNN layer. Formally, the representation at layer l is computed as:

$$Z^{(l)} = \text{MPNN}_l(Z^{(l-1)}, A) + Z^{(0)}. \quad (9)$$

This approach keeps access to the original node attributes throughout the network, preventing them from being diluted by multiple

Table 1: Summary of Convolutional Layer Characteristics

Convolution Type	Core Characteristics	Benefits	Drawbacks
GCN [11]	Uses spectral-based normalization for balanced aggregation	Balances node degree differences; robust and reliable	Limited flexibility due to fixed normalization
GraphSAGE [6]	Aggregates raw neighbor features using mean aggregator	Simpler aggregation; efficient on certain tasks	Weaker sensitivity to graph structure variations
GAT [24]	Employs attention mechanism for weighted aggregation	Effective on graphs with heterogeneous connectivity	High computational cost; prone to overfitting
GIN [31]	Incorporates MLP to enhance structural expressiveness	Highly expressive; strong on distinguishing structural details	Higher risk of overfitting, especially on smaller datasets

aggregation steps. This strategy is also used in architectures like GCNII [4] to help train very deep graph neural networks.

Non-Linear Activation (and its strategic absence). Section 4.1 highlighted that inner products of MPNN-derived embeddings can capture pairwise relationships. However, standard GNN designs often apply non-linear activations after convolution operation, resulting in updates like $H^{(l+1)} = \sigma(\text{Conv}_{l+1}(H^{(l)}, A))$. Such intermediate non-linearities can disrupt the direct structural information encoded in dot products. **Therefore, we strategically remove non-linear activations between sequential MPNN layers.** Each layer therefore performs a linear transformation. This approach is similar in principle to linear GNNs like SGC [30], where the update rule is $Z^{(l+1)} = \text{Conv}_{l+1}(Z^{(l)}, A)$. Stacking these linear layers allows the final encoder output to keep structural properties through inner products. The non-linearity is then introduced in the decoder stage. Several other recent works have also effectively used linear propagation for link prediction, including LightGCN [8], HL-GNN [33], YinYanGNN [27], and MPLP [5].

After the encoder produces node embeddings, the **decoder** can use the dot product followed by a sigmoid function to predict edge likelihoods. A more expressive alternative is to use an MLP, which can learn non-linear interactions between node embeddings. This is especially important if the encoder’s MPNN layers are linear, as the MLP in the decoder can then introduce the needed non-linear transformations to model complex relationships. **Similar to their use in the encoder’s MPNN layers, initial residual connections also help in training deeper MLPs in the decoder.** They help ensure stable training and effective information flow through the predictor’s layers.

4.2.3 Revisiting Standard Hyperparameter Settings. Beyond the specific architectural components, hyperparameters like **network depth** and **hidden dimension** are key in determining a GAE’s practical performance. Traditional GAEs often use conservative values for these parameters. This can result in insufficient model capacity, risking underfitting on large graphs and thus underestimating their true potential. Therefore, a careful re-evaluation of standard choices for hidden dimension and network depth is needed to correctly scale the GAE’s learning capacity.

Network Depth. The depth of the network plays an important role in determining its ability to capture complex patterns. However, GNNs have challenges with increasing depth, especially over-smoothing [13]. To address the challenge, we adopt the following approach: **our strategy uses shallow MPNN encoder layers yet deep MLP decoder layers.** This design allows the model to retain

high expressive power because the MLP learns complex relational patterns independently.

Hidden Dimension. A model’s capacity is closely linked to its hidden dimension size. However, some previous GNN studies have used relatively small dimensions (e.g., NCN [26] using a dimension of only 64 for ogbl-collab). While this reduces computational cost, such limited capacity can greatly underestimate a model’s actual performance. **Therefore, we use a sufficiently large hidden dimension to capture the complexities in large graphs.**

These observations highlight the need to go beyond default or overly conservative settings for network depth and hidden dimension. Careful, dataset-specific tuning of these hyperparameters is important for maximizing the performance of GAEs.

5 EXPERIMENTS

In this section, we present a detailed evaluation of our proposed model. This evaluation has three parts: (1) experimental setup (datasets, baselines, configurations), (2) main results comparing our model against SOTA baselines across multiple datasets, and (3) an ablation study on component contributions and hyperparameter settings. These experiments validate the effectiveness, scalability, and robustness of our approach on several real-world benchmarks.

5.1 Experiment Setup

Datasets We evaluate our model on three datasets from Planetoid [21]: Cora, Citeseer, and Pubmed; and four datasets from OGB [9]: ogbl-collab, ogbl-ddi, ogbl-ppa, and ogbl-citation2.

Baselines. We use the official OGB results for GAE as baselines. For a broader comparison, we also include heuristic methods such as Common Neighbors (CN) [2], Adamic-Adar (AA) [1], and Resource Allocation (RA) [36], as well as GNN models like SEAL [34], NeoGNN [32], NBFNet [38], BUDDY [3], NCN [26] and MPLP+ [5]. Baseline results are taken from three established studies [5, 9, 26].

Experiment settings. For the Planetoid datasets, we use a 70%-10%-20% train-validation-test split and evaluate performance using Hits@100 following prior works. For OGB datasets, we use the official data splits and evaluation metrics. **Guided by the input representation strategy, our main Optimized GAE model incorporates learnable node embeddings for the ogbl-ddi, ogbl-ppa, and ogbl-citation2 datasets.** Further experimental details are in Appendix A. Noted on ogbl-collab, different evaluation strategies have been used in previous work. Some studies [3, 5, 9, 26, 32, 34] include validation edges only during test time.

Table 2: Performance comparison. Metrics include Hits@100, Hits@50, Hits@20, and MRR. The best results are highlighted in bold, and the second-best are underlined. "OOM" indicates Out of Memory. "-" means not reported.

Metric	Cora Hits@100	Citeseer Hits@100	Pubmed Hits@100	Collab Hits@50	PPA Hits@100	Citation2 MRR	DDI Hits@20
CN	33.92 ± 0.46	29.79 ± 0.90	23.13 ± 0.15	56.44 ± 0.00	27.65 ± 0.00	51.47 ± 0.00	17.73 ± 0.00
AA	39.85 ± 1.34	35.19 ± 1.33	27.38 ± 0.11	64.35 ± 0.00	32.45 ± 0.00	51.89 ± 0.00	18.61 ± 0.00
RA	41.07 ± 0.48	33.56 ± 0.17	27.03 ± 0.35	64.00 ± 0.00	49.33 ± 0.00	51.98 ± 0.00	27.60 ± 0.00
SEAL	81.71 ± 1.30	83.89 ± 2.15	75.54 ± 1.32	64.74 ± 0.43	48.80 ± 3.16	87.67 ± 0.32	30.56 ± 3.86
NBFnet	71.65 ± 2.27	74.07 ± 1.75	58.73 ± 1.99	OOM	OOM	OOM	4.00 ± 0.58
Neo-GNN	80.42 ± 1.31	84.67 ± 2.16	73.93 ± 1.19	57.52 ± 0.37	49.13 ± 0.60	87.26 ± 0.84	63.57 ± 3.52
BUDDY	88.00 ± 0.44	92.93 ± 0.27	74.10 ± 0.78	65.94 ± 0.58	49.85 ± 0.20	87.56 ± 0.11	78.51 ± 1.36
NCN	89.05 ± 0.96	91.56 ± 1.43	<u>79.05 ± 1.16</u>	64.76 ± 0.87	61.19 ± 0.85	88.09 ± 0.06	<u>82.32 ± 6.10</u>
MPLP+	-	-	-	66.99 ± 0.40	<u>65.24 ± 1.50</u>	90.72 ± 0.12	-
GAE(GCN)	66.79 ± 1.65	67.08 ± 2.94	53.02 ± 1.39	47.14 ± 1.45	18.67 ± 1.32	84.74 ± 0.21	37.07 ± 5.07
GAE(SAGE)	55.02 ± 4.03	57.01 ± 3.74	39.66 ± 0.72	54.63 ± 1.12	16.55 ± 2.40	82.60 ± 0.36	53.90 ± 4.74
Optimized-GAE	<u>88.17 ± 0.93</u>	<u>92.40 ± 1.23</u>	80.09 ± 1.72	<u>66.11 ± 0.35</u>	78.41 ± 0.83	<u>88.74 ± 0.06</u>	94.43 ± 0.57

Table 3: Side-by-side comparison of reported performance of NCN and performance after applying our optimization techniques(denoted with *).

Metric	Cora Hits@100	Citeseer Hits@100	Pubmed Hits@100	Collab Hits@50	PPA Hits@100	Citation2 MRR	DDI Hits@20
NCN	89.05 ± 0.96	91.56 ± 1.43	79.05 ± 1.16	64.76 ± 0.87	61.19 ± 0.85	88.09 ± 0.06	82.32 ± 6.10
NCN*	89.07 ± 0.34	94.09 ± 0.40	81.27 ± 0.57	66.46 ± 0.67	73.91 ± 0.44	90.01 ± 0.08	92.84 ± 0.70
Improvement	(↑ 0.02)	(↑ 2.53)	(↑ 2.22)	(↑ 1.70)	(↑ 12.72)	(↑ 1.92)	(↑ 10.46)
GCN	66.79 ± 1.65	67.08 ± 2.94	53.02 ± 1.39	47.14 ± 1.45	18.67 ± 1.32	84.74 ± 0.21	37.07 ± 5.07
Optimized-GAE	88.17 ± 0.93	92.40 ± 1.23	80.09 ± 1.72	66.11 ± 0.35	78.41 ± 0.83	88.74 ± 0.06	94.43 ± 0.57
Improvement	(↑ 21.38)	(↑ 25.32)	(↑ 27.07)	(↑ 18.97)	(↑ 59.74)	(↑ 4.00)	(↑ 57.36)

Others [27, 29, 33] add the validation set to the training data, following current OGB guidelines. For our main results, we use the first strategy to align with the most common approach in the literature.

5.2 Main Results

The main results are presented in Table 2. Our model achieves SOTA on 3 datasets and top-2 on 4 datasets. The consistently strong performance reflects an average improvement of **91.5%** over the original GAE baseline. For instance, on the structure-reliant ogbl-ppa and ogbl-ddi datasets, where our input representation technique is particularly effective, performance improves from 18.67% to **78.41%** and from 37.07% to **94.43%**. Furthermore, Optimized-GAE shows an average improvement of **6.4%** over NCN [26], a competitive SOTA model, surpassing it on six out of seven datasets. Notably, on ogbl-ppa, our model's Hits@100 score of **78.41%** not only exceeds the strong MPLP+ baseline by a significant **20.2%** margin but also outperforms the OGB leaderboard leader by **2.4%**. These results support our main claim: a properly optimized GAE can match or exceed the performance of current models that use more complex methods, validating GAE's potential in current link prediction tasks.

Additionally, as many recent models use GAE as their foundation, our optimization techniques can also be applied to improve

their performance. Table 3 shows the results for the NCN model when improved with our techniques, **demonstrating a clear and consistent improvement in its performance**. This highlights the broader impact of our methods for improving general GNNs.

5.3 Ablation Study

In this section, we conduct a comprehensive ablation study to validate the techniques described in Section 4. This study highlights the importance of the proposed techniques and offers a deeper understanding of how they enhance the model's effectiveness.

5.3.1 Input Nodes Representations. The choice of input representations is fundamental to the Optimized GAE. This involves selecting between raw node features and learnable embeddings based on dataset characteristics, and ensuring that learnable embeddings are well-initialized. The following observations support these ideas:

Observation 1: The choice to use raw features (RF) alone or augment with learnable embeddings (LE) is mainly guided by the informativeness of raw features relative to the structure.

Explanation: Table 4 clearly supports this. A higher $I_{S/F}$ index typically indicates that LE are more beneficial. For instance, on the

Table 4: Dataset Characteristics and Performance Impact of Input Representation Choices. This table details graph statistics and the performance of models configured with additional learnable embeddings (LE) or only raw features (RF). For DDI, which lacks node features, "raw features" are represented by all-ones embeddings. The $I_{S/F}$ index is calculated as $P_S/(P_S + P_F + \epsilon)$, where P_S is the performance of common neighbor heuristic, and P_F represents the performance of cosine similarity heuristic.

Characteristic	Cora	Citeseer	Pubmed	Collab	PPA	Citation2	DDI
Metric	Hits@100	Hits@100	Hits@100	Hits@50	Hits@100	MRR	Hits@20
Perf. with LE	84.25 \pm 1.29	87.21 \pm 1.23	74.96 \pm 1.69	66.02 \pm 0.12	78.41 \pm 0.83	88.74 \pm 0.06	94.43 \pm 0.57
Perf. with RF	88.17 \pm 0.93	92.40 \pm 1.23	80.09 \pm 1.72	66.11 \pm 0.35	21.37 \pm 0.16	84.74 \pm 0.21	2.01 \pm 1.14 ²
Node count	2,708	3,327	18,717	235,868	576,289	2,927,963	4,267
Avg. Degree	3.90	2.81	4.73	5.45	52.62	10.44	312.84
$I_{S/F}$ Index	0.394	0.292	0.398	0.682	1.000	0.741	1.000

Table 5: Ablation study for Optimized-GAE, evaluating key design choices covering: (1) Input Representation; (2) Convolution Layers; (3) Layer Design (impact of residual connections and MPNN encoder linearity).

Metric	Cora Hits@100	Citeseer Hits@100	Pubmed Hits@100	DDI Hits@20	Collab Hits@50
Optimized-GAE	88.17 \pm 0.93	92.40 \pm 1.23	80.09 \pm 1.72	94.43 \pm 0.57	66.11 \pm 0.35
Input Representation					
all-ones learnable embedding	32.93 \pm 2.73	31.08 \pm 2.52	32.89 \pm 1.23	2.13 \pm 1.46	65.16 \pm 0.14
random learnable embedding	32.12 \pm 2.56	30.99 \pm 3.36	48.72 \pm 2.12	13.84 \pm 1.93	65.77 \pm 0.53
fixed orthogonal embedding	80.02 \pm 2.31	73.81 \pm 0.89	75.88 \pm 0.84	77.61 \pm 1.55	65.88 \pm 0.16
Convolution Layers					
SAGE	80.04 \pm 3.40	89.12 \pm 0.40	80.12 \pm 0.43	72.46 \pm 11.23	65.28 \pm 0.35
GAT	80.99 \pm 3.97	87.71 \pm 2.29	81.93 \pm 1.49	89.45 \pm 2.01	66.01 \pm 0.11
GIN	82.52 \pm 0.90	68.02 \pm 1.83	83.00 \pm 0.60	96.45 \pm 0.42	67.94 \pm 0.43
Layer Design: Residuals & Linearity					
No Residual in MPNN	69.95 \pm 5.77	79.52 \pm 2.48	78.46 \pm 1.39	71.12 \pm 1.52	66.11 \pm 0.16
No Residual in MLP	84.45 \pm 2.29	91.21 \pm 1.23	80.17 \pm 1.88	94.02 \pm 1.05	65.46 \pm 1.34
No Residual in Both	29.10 \pm 18.41	78.51 \pm 1.12	78.10 \pm 1.09	26.4 \pm 2.59	65.46 \pm 1.34
Nonlinear MPNN Layers	83.47 \pm 0.77	67.15 \pm 1.97	80.56 \pm 1.33	66.77 \pm 3.45	65.68 \pm 0.63

ogbl-ppa dataset, which lacks informative raw features ($I_{S/F} \approx 1.000$), using LE substantially improves performance from approximately 21.37 to 78.41. Conversely, for a feature-rich dataset like Citeseer ($I_{S/F} \approx 0.292$), using its strong RF alone gives a result of 92.40, which is better than the 87.21 achieved if LE are used. While the overall success of LE also depends on graph size and density (see Observation 2), the $I_{S/F}$ index provides an important first assessment. It helps determine if the node features are sufficient or if the model needs to focus more on the graph structure.

Observation 2: Besides the $I_{S/F}$ index, graph size (number of nodes) and density (average degree) are key factors in determining whether LE can be beneficial.

Explanation: The effect of graph size and density on LE effectiveness, even with similar feature informativeness, is clear when comparing ogbl-collab and ogbl-citation2. While both datasets exhibit similar $I_{S/F}$ indices, ogbl-citation2 is significantly larger and denser than ogbl-collab. On ogbl-citation2, LEs offer a clear advantage over RF. However, on the smaller and sparser ogbl-collab, RF performance is similar to that of LE. This suggests that larger graph scale and higher density better support LE.

Observation 3: Orthogonal initialization of learnable node embeddings is a significantly more effective starting point compared to arbitrary initializations.

Explanation: The major impact of initialization is clear from Table 5. For instance, while Optimized-GAE uses LEs with an orthogonal initialization and achieves a Hits@20 score of 94.43 on ogbl-ddi, performance drops sharply with less structured initializations. Specifically, using an "all-ones initialization," where initial embedding vectors are all ones, results in a score of only 2.13. Similarly, using "random initialization," where embeddings are initialized with values selected uniformly from $[-1, 1]$ (a method likely to break any initial orthogonality), greatly reduces performance to 13.84. This large drop in performance highlights the importance of orthogonal initialization. Notably, even after training, these learnable embeddings often remain close to orthogonal. Specifically, on ogbl-ddi, the average absolute cosine similarity was 0.03 (std. dev. 0.04) before training and 0.07 (std. dev. 0.07) after training. This reflects the important role of common neighbor information in link prediction, as discussed in Section 4.1.

Observation 4: The adaptability offered by making node embeddings *learnable* is important for achieving best performance, and is better than using fixed embedding strategies.

Explanation: Table 5 also shows the benefits of learnability. While using ‘fixed orthogonal embeddings’ (initialized orthogonally but not updated during training) on ogbl-ddi achieves a Hits@20 score of 77.61, this is much lower than the 94.43 achieved by the full Optimized-GAE with learnable embeddings. This performance gap highlights that allowing the embeddings to be fine-tuned enables the model to use more than just common neighbor information and capture detailed representations specific to the graph structure.

5.3.2 Key Architectural Modules of Graph Autoencoders. Beyond input representation, the design of the GAE’s architectural components critically influences its performance. These include the choice of graph convolutional operation, the strategy for incorporating residual connections, and the handling of non-linearities within the network. The following observations, based on the ablation results in Table 5, validate our design principles for these modules.

Observation 5: While GCN serve as a effective default for the Optimized-GAE, alternative convolutional architectures exhibit varying performance trade-offs, underscoring the importance of layer selection tailored to dataset characteristics.

Explanation: Table 5(section “Convolution Layers”) compares the performance of Optimized-GAE (which uses GCN by default) against variants employing SAGE, GAT, and GIN. While GCN provides strong performance across datasets, alternatives show varied results. For example, GIN can achieve higher performance on large scale benchmarks like ogbl-ddi (96.45) by potentially capturing finer-grained structural details, but it may overfit on small graphs like CiteSeer (68.02). SAGE often trails GCN, particularly on datasets where degree normalization is beneficial. GAT also generally performs slightly below GCN. These findings affirm GCN as a generally well-performing choice, while highlighting that specific dataset properties might favor other architectures, emphasizing the need for dataset-specific tuning if deviating from GCN.

Observation 6: Using initial residual connections in both the MPNN encoder and the MLP decoder is key for stable training and effective information propagation, significantly improving GAE performance.

Explanation: The role of residual connections is confirmed by ablations in Table 5(section “Layer Design”). Removing initial residual connections from the encoder causes a substantial performance drop on all datasets. This shows their importance for keeping initial node information during the encoding process. While removing residuals from the decoder has a less dramatic impact on some datasets, it can still harm results (e.g., Cora performance drops to 84.45). Importantly, removing residual connections from both components results in a severe drop in performance (e.g., ogbl-ddi to 26.4). Together, these findings highlight that residual connections are necessary for high-performing GAE models.

Observation 7: Removing non-linear activation functions from the intermediate layers of the MPNN encoder to keep linear message propagation until the decoder stage—is a key

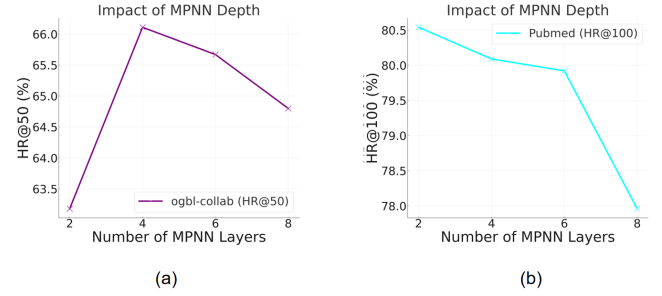


Figure 3: Impact of MPNN layer depth on performance for (a) ogbl-collab and (b) Pubmed.

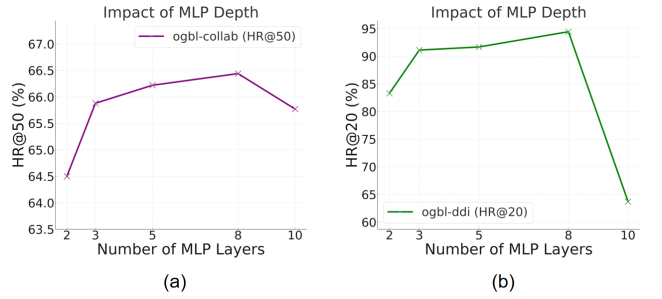


Figure 4: Impact of MLP layer depth on performance for (a) ogbl-collab and (b) ogbl-ddi.

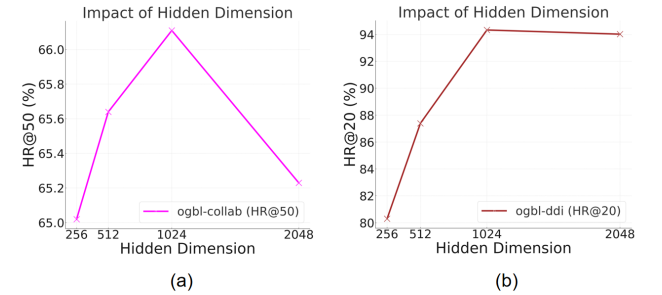


Figure 5: Impact of hidden dimension on performance for (a) ogbl-collab and (b) ogbl-ddi.

factor for preserving structural information and achieving better link prediction performance.

Explanation: The significant advantage of using linear encoder layers is supported by the “Nonlinear MPNN Layers” ablation presented in Table 5 (section “Layer Design”). When non-linear activation functions are added back between the MPNN layers in the Optimized-GAE’s encoder, performance consistently and often substantially drops on multiple datasets. For example, on ogbl-ddi, the result falls from 94.43 to 66.77. These results strongly support our design choice of using linear propagation in the encoder. This allows the model to effectively capture and keep pairwise relational signals and structural information, as discussed in Section 4.1.

5.3.3 Hyperparameter Tuning: Network Depth and Hidden Dimension. Beyond architectural choices, the careful tuning of hyperparameters like network depth and hidden dimension, as emphasized in Section 4.2.3, is key for achieving the GAE’s full potential. The following observations support our strategies for these settings:

Table 6: Comparison of time complexity per training batch and total runtime (seconds) on evaluation sets across various models and datasets. Here, B denotes batch size, and h the hashing sketch size for BUDDY and MPLP+. Detailed complexity analysis is provided in Appendix B.

Model	Complexity	ddi	collab
Optimized-GAE	$O(E d + Bd^2)$	0.12	0.07
SEAL	$O(B E d + B V d^2)$	209	1080
BUDDY	$O(E d + E h + Bd^2 + Bh)$	57	3.3
MPLP+	$O(E d + E h + V d^2 + Bd^2)$	0.19	0.20

Observation 8: Optimal GAE performance is achieved through a strategy that employs shallow MPNN encoder layers to mitigate oversmoothing, complemented by deeper MLP decoder layers which enhance model capacity.

Explanation: The impact of MPNN depth is illustrated in Figure 3. Performance generally peaks when using 2-4 MPNN layers, with further increases often leading to diminishing returns or a decline, likely due to oversmoothing. This supports our approach of using a relatively shallow MPNN encoder. Conversely, as shown in Figure 4, increasing the depth of the MLP decoder layers consistently improves performance up to an optimal point where the model sufficiently captures the data complexity. This presents the benefit of using deeper MLPs in the decoder to model complex interactions.

Observation 9: Using an appropriately sized hidden dimension is important for model capacity; GAE performance generally improves with larger dimensions until the benefits lessen or computational trade-offs become too large.

Explanation: Figure 5 shows the effect of varying the hidden dimension. Performance typically increases as d is enlarged, allowing the model to represent more complex patterns. For example, on ogbl-ddi, Hits@20 significantly improves when moving from smaller dimensions to $d = 1024$. However, beyond a certain size (e.g., $d = 1024$ for ogbl-collab), the gains may lessen or even decrease. This highlights the need to choose a suitable hidden dimension that balances capacity with efficiency and helps prevent overfitting from too many parameters.

6 EFFICIENCY

In addition to its strong performance, Optimized-GAE is also highly scalable due to its simple architecture. Models like GAE do not require explicit calculation of pairwise information, which gives them an inherent efficiency advantage over models that use complex methods to include pairwise information. For example, SEAL requires subgraph extraction and DRNL calculation for each node [34], while BUDDY precomputes subgraph-related information and structural features for each batch [3], causing significant overhead. Table 6 compares the time complexity per training batch and the actual runtime per training epoch on the same machine, highlighting that our GAE-based approach offers scalability benefits over models with complex pairwise methods, even when using a large hidden dimension and deeper layers.

7 CONCLUSION

This work demonstrates that a holistically optimized GAE can achieve SOTA link prediction performance, rivaling sophisticated contemporary models often with superior efficiency. Our success, achieved through systematic and validated enhancements to GAE’s input representation strategies, core architectural designs, and meticulous hyperparameter tuning, underscores the critical importance of re-evaluating simple baseline models. This study not only provides a robustly tuned baseline and practical design guidelines but more broadly highlights that advancements in graph learning can significantly benefit from the thorough understanding and refinement of well-established architectures.

A EXPERIMENTAL DETAILS

Datasets To evaluate the performance of Optimized-GAE, we leverage a variety of widely used benchmark datasets. These datasets are sourced from two established repositories: Planetoid [21] and OGB [9]. From the Planetoid collection, we utilize Cora, Citeseer, and Pubmed, while the OGB repository provides ogbl-collab, ogbl-ddi, ogbl-ppa, and ogbl-citation2. Together, these datasets cover a range of graph structures and relationship patterns, enabling a comprehensive evaluation of model performance.

Computing infrastructure Our model is built with DGL [25] and PyTorch [20]. Experiments are conducted on Nvidia 4090 GPUs, except for the ogbl-citation2 dataset, which is run on Nvidia A800 GPUs due to its higher computational requirements.

Training process We set the upper bound for training epochs to 500, slightly higher than previous settings, as we observed that performance continues to improve on certain datasets up to this limit. This extended training duration is feasible due to the relatively high training speed of GAE. A 1:3 negative sampling ratio was employed (three negative edges per positive edge). All results are computed from runs conducted with 5 different random seeds.

Model Hyperparameters We tune the hyperparameters using a bayesian optimization, selecting values that yield the best validation performance. Table 7 summarizes the hyperparameter settings.

B COMPLEXITY ANALYSIS

First, we analyze the time complexity of Optimized-GAE. A typical MPNN layer such as a GCN involves a round of message passing and a nonlinear transformation. This results in a total time complexity of $O(|E|d + |V|d^2)$. However, Optimized-GAE skips the nonlinear transformation, reducing the complexity to $O(|E|d)$. Additionally, training involves running an MLP on a batch of edges with a complexity of $O(Bld^2)$. For space complexity, MPNN layers have $O(|E| + |V|d)$, where the second term corresponds to node embeddings. MLP predictors have $O(Bd + ld^2)$, with the first term for edge embeddings and the second for the weight matrix.

We further analyze the time complexity of recent models in Table 6. For each link, SEAL extracts a subgraph and runs an MPNN, leading to a batch complexity of $O(B|E|d + B|V|d^2)$. BUDDY only runs a lightweight MPNN on the full graph once instead and computes hashing sketches, resulting in a complexity of $O(|E|d + |E|h)$, followed by an MLP predictor with complexity $O(Bd^2 + Bh)$. MPLP+ propagates orthogonal sketches in addition to the standard GAE model, introducing an extra complexity of $O(|E|h)$.

Table 7: Hyperparameter Search Ranges and Selected Values for Each Dataset

Hyperparameter	Search Range	Cora	Citeseer	Pubmed	ogbl-ddi	ogbl-collab	ogbl-ppa	ogbl-citation2
Learning Rate (lr)	$\{5 \times 10^{-4}, 10^{-4}, 5 \times 10^{-4}\}$	5×10^{-3}	10^{-3}	10^{-3}	10^{-3}	5×10^{-4}	5×10^{-4}	5×10^{-4}
MPNN Layers	$\{2, 3, 4\}$	4	4	4	2	4	2	3
Hidden Dimension	$\{256, 512, 1024\}$	1024	1024	512	1024	512	512	256
Batch Size	$[2048, 65536]$	2048	4096	4096	8192	16384	65536	65536
Dropout	$\{0.2, 0.4, 0.6\}$	0.6	0.6	0.4	0.6	0.2	0.2	0.2
Mask Input	$\{\text{True}, \text{False}\}$	True	True	True	True	False	False	False
Normalization	$\{\text{True}, \text{False}\}$	True	True	True	False	True	False	True
MLP Layers	$\{2, 4, 5, 8\}$	4	2	2	8	5	5	5

ACKNOWLEDGMENTS

We thank the anonymous reviewers of CIKM 2025 for their time and insightful feedback, which helped improve this paper.

GENAI USAGE DISCLOSURE

Generative AI (GenAI) tools were utilized in the preparation of this manuscript to assist with coding and language polishing. The core research ideas, experimental design, analysis, and the overall drafting and writing of the paper were conducted by the authors without the involvement of GenAI.

REFERENCES

- [1] Lada A Adamic and Eytan Adar. 2003. Friends and neighbors on the web. *Social networks* 25, 3 (2003), 211–230.
- [2] Albert-László Barabási and Réka Albert. 1999. Emergence of scaling in random networks. *science* 286, 5439 (1999), 509–512.
- [3] Benjamin Paul Chamberlain, Sergey Shirobokov, Emanuele Rossi, Fabrizio Frasca, Thomas Markovich, Nils Yannick Hammerla, Michael M. Bronstein, and Max Hansmire. 2023. Graph Neural Networks for Link Prediction with Subgraph Sketching. In *The Eleventh International Conference on Learning Representations, ICLR 2023, May 1–5, 2023*. OpenReview.net, Kigali, Rwanda. <https://openreview.net/forum?id=m1oqEOAozQU>
- [4] Ming Chen, Zhewei Wei, Zengfeng Huang, Bolin Ding, and Yaliang Li. 2020. Simple and Deep Graph Convolutional Networks. In *Proceedings of the 37th International Conference on Machine Learning, ICML 2020, 13–18 July 2020, Virtual Event (Proceedings of Machine Learning Research, Vol. 119)*. PMLR, 1725–1735. <http://proceedings.mlr.press/v119/chen20v.html>
- [5] Kaiwen Dong, Zhichun Guo, and Nitesh V. Chawla. 2023. Pure Message Passing Can Estimate Common Neighbor for Link Prediction. *CoRR* abs/2309.00976 (2023). doi:10.48550/ARXIV.2309.00976 arXiv:2309.00976
- [6] Will Hamilton, Zitao Ying, and Jure Leskovec. 2017. Inductive representation learning on large graphs. *Advances in neural information processing systems* 30 (2017), 1024–1034.
- [7] Kaiming He, Xiangyu Zhang, Shaoqing Ren, and Jian Sun. 2016. Deep Residual Learning for Image Recognition. In *2016 IEEE Conference on Computer Vision and Pattern Recognition, CVPR 2016, June 27–30, 2016*. IEEE Computer Society, Las Vegas, NV, USA, 770–778. doi:10.1109/CVPR.2016.90
- [8] Xiangnan He, Kuan Deng, Xiang Wang, Yan Li, Yong-Dong Zhang, and Meng Wang. 2020. LightGCN: Simplifying and Powering Graph Convolution Network for Recommendation. In *Proceedings of the 43rd International ACM SIGIR conference on research and development in Information Retrieval, SIGIR 2020, Virtual Event, July 25–30, 2020*. Jimmy X. Huang, Yi Chang, Xueqi Cheng, Jaap Kamps, Vanessa Murdock, Ji-Rong Wen, and Yiqun Liu (Eds.). ACM, China, 639–648. doi:10.1145/3397271.3401063
- [9] Weihua Hu, Matthias Fey, Marinka Zitnik, Yuxiao Dong, Hongyu Ren, Bowen Liu, Michele Catasta, and Jure Leskovec. 2020. Open graph benchmark: Datasets for machine learning on graphs. *Advances in neural information processing systems* 33 (2020), 22118–22133.
- [10] Thomas N. Kipf and Max Welling. 2016. Variational Graph Auto-Encoders. *CoRR* abs/1611.07308 (2016). arXiv:1611.07308 <http://arxiv.org/abs/1611.07308>
- [11] Thomas N. Kipf and Max Welling. 2017. Semi-Supervised Classification with Graph Convolutional Networks. In *5th International Conference on Learning Representations, ICLR 2017, April 24–26, 2017, Conference Track Proceedings*. OpenReview.net, Toulon, France. <https://openreview.net/forum?id=SJU4ayYgl>
- [12] Juanhui Li, Harry Shomer, Haitao Mao, Shenglai Zeng, Yao Ma, Neil Shah, Jiliang Tang, and Dawei Yin. 2024. Evaluating graph neural networks for link prediction: Current pitfalls and new benchmarking. *Advances in Neural Information Processing Systems* 36 (2024).
- [13] Qimai Li, Zhichao Han, and Xiao-Ming Wu. 2018. Deeper Insights Into Graph Convolutional Networks for Semi-Supervised Learning. In *Proceedings of the Thirty-Second AAAI Conference on Artificial Intelligence (AAAI-18), the 30th innovative Applications of Artificial Intelligence (IAAI-18), and the 8th AAAI Symposium on Educational Advances in Artificial Intelligence (EAAI-18), February 2–7, 2018*, Sheila A. McIlraith and Kilian Q. Weinberger (Eds.). AAAI Press, New Orleans, Louisiana, USA, 3538–3545. doi:10.1609/AAAI.V32I1.11604
- [14] Shuming Liang, Yu Ding, Zhidong Li, Bin Liang, Siqi Zhang, Yang Wang, and Fang Chen. 2024. Can GNNs Learn Link Heuristics? A Concise Review and Evaluation of Link Prediction Methods. *CoRR* abs/2411.14711 (2024). doi:10.48550/ARXIV.2411.14711 arXiv:2411.14711
- [15] Yuankai Luo, Lei Shi, and Xiao-Ming Wu. 2024. Classic GNNs are Strong Baselines: Reassessing GNNs for Node Classification. In *Advances in Neural Information Processing Systems 38: Annual Conference on Neural Information Processing Systems 2024, NeurIPS 2024, Vancouver, BC, Canada, December 10–15, 2024*, Amir Globersons, Lester Mackey, Danielle Belgrave, Angela Fan, Ulrich Paquet, Jakub M. Tomczak, and Cheng Zhang (Eds.). http://papers.nips.cc/paper_files/paper/2024/hash/b10ed15ff1aa864f1be3a75f1ffc021b-Abstract-Datasets_and_Benchmarks_Track.html
- [16] Yuankai Luo, Lei Shi, and Xiao-Ming Wu. 2025. Unlocking the Potential of Classic GNNs for Graph-level Tasks: Simple Architectures Meet Excellence. *CoRR* abs/2502.09263 (2025). doi:10.48550/ARXIV.2502.09263 arXiv:2502.09263
- [17] Li Ma, Haoyu Han, Juanhui Li, Harry Shomer, Hui Liu, Xiaofeng Gao, and Jiliang Tang. [n. d.]. Mixture of Link Predictors on Graphs. In *The Thirty-eighth Annual Conference on Neural Information Processing Systems*.
- [18] Haitao Mao, Juanhui Li, Harry Shomer, Bingheng Li, Wenqi Fan, Yao Ma, Tong Zhao, Neil Shah, and Jiliang Tang. 2023. Revisiting link prediction: A data perspective. *arXiv preprint arXiv:2310.00793* (2023).
- [19] Christopher Morris, Martin Ritzert, Matthias Fey, William L Hamilton, Jan Eric Lenssen, Gaurav Rattan, and Martin Grohe. 2019. Weisfeiler and leman go neural: Higher-order graph neural networks. In *Proceedings of the AAAI conference on artificial intelligence*, Vol. 33. 4602–4609.
- [20] Adam Paszke, Sam Gross, Francisco Massa, Adam Lerer, James Bradbury, Gregory Chanan, Trevor Killeen, Zeming Lin, Natalia Gimelshein, Luca Antiga, et al. 2019. Pytorch: An imperative style, high-performance deep learning library. *Advances in neural information processing systems* 32 (2019), 8024–8035.
- [21] Prithviraj Sen, Galileo Namata, Mustafa Bilgic, Lise Getoor, Brian Galligher, and Tina Eliassi-Rad. 2008. Collective classification in network data. *AI magazine* 29, 3 (2008), 93–93.
- [22] Harry Shomer, Yao Ma, Haitao Mao, Juanhui Li, Bo Wu, and Jiliang Tang. 2024. Lpformer: An adaptive graph transformer for link prediction. In *Proceedings of the 30th ACM SIGKDD Conference on Knowledge Discovery and Data Mining*. 2686–2698.
- [23] E. Amiri Souri, Roman Laddach, S. N. Karagiannis, Lazaros G. Papageorgiou, and Sophia Tsoka. 2022. Novel drug-target interactions via link prediction and network embedding. *BMC Bioinform.* 23, 1 (2022), 121. doi:10.1186/S12859-022-04650-W
- [24] Petar Velickovic, Guillem Cucurull, Arantxa Casanova, Adriana Romero, Pietro Liò, and Yoshua Bengio. 2018. Graph Attention Networks. In *6th International Conference on Learning Representations, ICLR 2018, April 30 – May 3, 2018, Conference Track Proceedings*. OpenReview.net, Vancouver, BC, Canada. <https://openreview.net/forum?id=rJXmpikCZ>
- [25] Minjie Wang, Lingfan Yu, Da Zheng, Quan Gan, Yu Gai, Zihao Ye, Mufei Li, Jinjing Zhou, Qi Huang, Chao Ma, Ziyue Huang, Qipeng Guo, Hao Zhang, Haibin Lin, Junbo Zhao, Jinyang Li, Alexander J. Smola, and Zheng Zhang. 2019. Deep Graph Library: Towards Efficient and Scalable Deep Learning on Graphs. *CoRR* abs/1909.01315 (2019). arXiv:1909.01315 <http://arxiv.org/abs/1909.01315>
- [26] Xiyuan Wang, Haotong Yang, and Muhan Zhang. 2024. Neural Common Neighbor with Completion for Link Prediction. In *The Twelfth International Conference on Learning Representations, ICLR 2024, May 7–11, 2024*. OpenReview.net, Vienna, Austria. <https://openreview.net/forum?id=sNFLN3itAd>
- [27] Yuxin Wang, Xiannian Hu, Quan Gan, Xuanjing Huang, Xipeng Qiu, and David Wipf. 2025. Efficient Link Prediction via GNN Layers Induced by Negative Sampling. *IEEE Trans. Knowl. Data Eng.* 37, 1 (2025), 253–264. doi:10.1109/TKDE.2024.3481015
- [28] Yakun Wang, Daixin Wang, Hongrui Liu, Binbin Hu, Yingcui Yan, Qiyang Zhang, and Zhiqiang Zhang. 2024. Optimizing Long-tailed Link Prediction in Graph Neural Networks through Structure Representation Enhancement. In *Proceedings of the 30th ACM SIGKDD Conference on Knowledge Discovery and Data Mining*. 3222–3232.
- [29] Zitao Wang, Yong Zhou, Litao Hong, Yuanhang Zou, Hanjing Su, and Shouzhi Chen. 2021. Pairwise Learning for Neural Link Prediction. *CoRR* abs/2112.02936 (2021). arXiv:2112.02936 <https://arxiv.org/abs/2112.02936>
- [30] Felix Wu, Amauri H. Souza Jr., Tianyi Zhang, Christopher Fifty, Tao Yu, and Kilian Q. Weinberger. 2019. Simplifying Graph Convolutional Networks. In *Proceedings of the 36th International Conference on Machine Learning, ICML 2019, 9–15 June 2019 (Proceedings of Machine Learning Research, Vol. 97)*, Kamalika Chaudhuri and Ruslan Salakhutdinov (Eds.). PMLR, Long Beach, California, USA, 6861–6871. <http://proceedings.mlr.press/v97/wu19e.html>
- [31] Keyulu Xu, Weihua Hu, Jure Leskovec, and Stefanie Jegelka. 2019. How Powerful are Graph Neural Networks?. In *7th International Conference on Learning Representations, ICLR 2019, May 6–9, 2019*. OpenReview.net, New Orleans, LA, USA. <https://openreview.net/forum?id=ryGs6iA5Km>
- [32] Seongjun Yun, Seoyoon Kim, Junhyun Lee, Jaewoo Kang, and Hyunwoo J Kim. 2021. Neo-gnns: Neighborhood overlap-aware graph neural networks for link prediction. *Advances in Neural Information Processing Systems* 34 (2021), 13683–13694.

- [33] Juzheng Zhang, Lanning Wei, Zhen Xu, and Quanming Yao. 2024. Heuristic Learning with Graph Neural Networks: A Unified Framework for Link Prediction. In *Proceedings of the 30th ACM SIGKDD Conference on Knowledge Discovery and Data Mining, KDD 2024, August 25–29, 2024*, Ricardo Baeza-Yates and Francesco Bonchi (Eds.). ACM, Barcelona, Spain, 4223–4231. doi:10.1145/3637528.3671946
- [34] Muhan Zhang and Yixin Chen. 2018. Link prediction based on graph neural networks. *Advances in neural information processing systems* 31 (2018).
- [35] Muhan Zhang and Yixin Chen. 2020. Inductive Matrix Completion Based on Graph Neural Networks. In *8th International Conference on Learning Representations, ICLR 2020, April 26–30, 2020*. OpenReview.net, Addis Ababa, Ethiopia. <https://openreview.net/forum?id=ByxxgCEYDS>
- [36] Tao Zhou, Linyuan Lü, and Yi-Cheng Zhang. 2009. Predicting missing links via local information. *The European Physical Journal B* 71 (2009), 623–630.
- [37] Jiong Zhu, Gaotang Li, Yao-An Yang, Jing Zhu, Xuehao Cui, and Danai Koutra. 2024. On the impact of feature heterophily on link prediction with graph neural networks. *arXiv preprint arXiv:2409.17475* (2024).
- [38] Zhaocheng Zhu, Zuobai Zhang, Louis-Pascal Khonneux, and Jian Tang. 2021. Neural bellman-ford networks: A general graph neural network framework for link prediction. *Advances in Neural Information Processing Systems* 34 (2021), 29476–29490.